Saudi Pharmaceutical Journal 28 (2020) 509–518

Contents lists available at ScienceDirect

Saudi Pharmaceutical Journal

journal homepage: www.sciencedirect.com

Original article

Liraglutide attenuates gefitinib-induced cardiotoxicity and promotes cardioprotection through the regulation of MAPK/NF-κB signaling pathways

Abdullah F. AlAsmari [a,*], Nemat Ali [a], Fawaz AlAsmari [a], Wael A. AlAnazi [a], Musaad A. AlShammari [a], Naif O. Al-Harbi [a], Ali Alhoshani [a], Homood M. As Sobeai [a], Mohammed AlSwayyed [b], Mohammed M. AlAnazi [a], Nader S. AlGhamdi [c]

[a] Department of Pharmacology and Toxicology, College of Pharmacy, King Saud University, Riyadh 11451, Saudi Arabia
[b] Department of Pathology, College of Medicine, King Saud University, Riyadh 11451, Saudi Arabia
[c] Department of Pharmacy Services, Prince Mohammed Bin Abdulaziz Hospital, Riyadh 14214, Saudi Arabia

ARTICLE INFO

Article history:
Received 6 January 2020
Accepted 3 March 2020
Available online 19 March 2020

Keywords:
Liraglutide
Cardiotoxicity
Gefitinib
Antioxidant
MAPK
Cardioprotection

ABSTRACT

Gefitinib is an effective treatment for patients with locally advanced non-small cell lung cancer. However, it is associated with cardiotoxicity that can limit its clinical use. Liraglutide, a glucagon-like peptide 1 receptor agonist, showed potent cardioprotective effects with the mechanism is yet to be elucidated. Therefore, this study aimed to determine the efficiency of liraglutide in protecting the heart from damage induced by gefitinib. Adult male Wistar rats were randomly divided into control group, liraglutide group (200 μg/kg by i.p. injection), gefitinib group (30 mg/kg orally) and liraglutide plus gefitinib group. After 28 days, blood and tissue samples were collected for histopathological, biochemical, gene and protein analysis. We demonstrated that gefitinib treatment (30 mg/kg) resulted in cardiac damage as evidenced by histopathological studies. Furthermore, serum Creatine kinase-MB (CK-MB), N-terminal pro B-type natriuretic peptide (NT-proBNP) and cardiac Troponin-I (cTnI) were markedly elevated in gefitinib group. Pretreatment with liraglutide (200 μg/kg), however, restored the elevation in serum markers and diminished gefitinib-induced cardiac damage. Moreover, liraglutide improved the gene and protein levels of anti-oxidant (superoxide dismutase) and decreased the oxidative stress marker (NF-κB). Mechanistically, liraglutide offered protection through upregulation of the survival kinases (ERK1/2 and Akt) and downregulation of stress-activated kinases (JNK and P38). In this study, we provide evidence that liraglutide protects the heart from gefitinib-induced cardiac damage through its anti-oxidant property and through the activation of survival kinases.

1. Introduction

It is reported that most of the complex living organisms respond coordinately to different extracellular stimuli in order to maintain normal biological functions, such as endo and exocrine secretion, neurotransmission, smooth muscle contraction, inflammatory responses, modulation of cardiac functions and pain, by activating specific signaling cascades and intracellular programs, such as mitogen activated protein kinases (MAPKs). By engaging and activating MAPKs, cells can regulate and control embryogenesis, cell proliferation, differentiation and death, gene expression, metabolism and survival (Chen et al., 2001; Kyriakis and Avruch, 2001; Roux and Blenis, 2004). One of the main extracellular signals transducer is receptor tyrosine kinases (RTKs), which upon activation

Abbreviations: NT-proBNP, N-terminal pro B-type natriuretic peptide; CK-MB, Creatine kinase-MB; cTnI, cardiac Troponin-I; NF-κB, Nuclear factor kappa B; MAPK, Mitogen activated protein kinase; ERK1/2, Extracellular signal–regulated kinase 1/2; Akt, Protein kinase B; JNK, C-Jun N-terminal kinase; LIRA, Liraglutide; GEF, Gefitinib; RTKs, Receptor tyrosine kinases; RTKIs, Receptor tyrosine kinases inhibitors; EGFR, Epidermal growth factor receptor; LDH, Lactate dehydrogenase; GLP-1, Glucagon-like peptide-1.

* Corresponding author at: Dept. of Pharmacology & Toxicology, College of Pharmacy, P.O. Box 2457, Riyadh 11451, Saudi Arabia.
E-mail address: afalasmari@ksu.edu.sa (A.F. AlAsmari).

Peer review under responsibility of King Saud University.

Production and hosting by Elsevier

https://doi.org/10.1016/j.jsps.2020.03.002
1319-0164/

lead to intracellular activation of different signaling pathways that control cell metabolism, growth and apoptosis. Findings from several reports revealed that overexpression or mutation of the RTKs is associated with the development of different types of cancer (Chen et al., 2008; Hervent and De Keulenaer, 2012; Orphanos et al., 2009; Schlessinger, 2000, 2014). These findings fostered the field of cancer research to develop new and effective anticancer agents that target the activation of RTKs. Ultimately, receptor tyrosine kinases inhibitors (RTKIs) were developed to block and diminish the activation of RTKs. Currently, drugs of this class are widely used to treat different types of cancer (Jiao et al., 2018; Montor et al., 2018).

Gefitinib (GEF) is a small molecule that selectively, reversibly and competitively inhibits RTKs activation, specifically epidermal growth factor receptor (EGFR) activation, resulting in inhibition of tumor growth, proliferation and differentiation and eventually induction of apoptosis in cancerous cells (Chen et al., 2008; Hervent and De Keulenaer, 2012; Segovia-Mendoza et al., 2015). Therefore, it is effective in treating NSCLC (non-small cell lung cancer). Since RTKIs inhibit the activation of RTKs in both normal and cancerous cells, RTKIs treatment can result in many but serious side effects (Kazandjian et al., 2016; Krawczyk et al., 2017; Segovia-Mendoza et al., 2015; Yang et al., 2017). It has been reported that GEF treatment was associated with recurrent myocardial infarction in patient with metastatic carcinoid tumor (Lynch et al., 2011). In that study, Lynch and colleagues reported that GEF treatment induced cardiomyopathy in 56-year-old patient with EGFR-mutated NSCLC. Furthermore, Korashy and his colleagues reported that in-vitro and in-vivo treatment with GEF resulted in significant increase in the apoptotic genes, oxidative stress markers, cardiac enzymes (LDH and CK-MB), hypertrophic genes and formation of reactive oxygen species (ROS) (Korashy et al., 2016). Although GEF treatment is associated with the development of cardiac toxicity, the exact mechanism is to be further investigated due to the limited information available about the mechanism of cardiotoxicity induced by GEF.

Recent studies demonstrated that liraglutide (LIRA) treatment was associated with lower risk of cardiovascular diseases and death among patients with type 2 diabetes (Marso et al., 2016). Moreover, LIRA treatment led to an improvement in the cardiac function in response to myocardial infarction in mice (Noyan-Ashraf et al., 2009). LIRA is a synthetic glucagon-like peptide-1 (GLP-1) receptor agonist that is used to effectively treat patients with type 2 diabetes mellitus either as monotherapy or as combination with other antidiabetic medications (Deng et al., 2018; Garber, 2011; Guo et al., 2018). Despite the documented hypoglycemic effect of LIRA, different studies confirmed that LIRA has an anti-inflammatory and antioxidant effects (Briyal et al., 2014; Zhang et al., 2018). Nevertheless, whether LIRA offers protection against GEF-induced cardiotoxicity is still unclear. Therefore, the main aim of the current study is to investigate the mechanism of toxicity induced by GEF and if LIRA pretreatment can mitigate GEF-induced cardiotoxicity *in-vivo*.

2. Materials and methods

2.1. Animals

The breeding and experimental protocols described in this study were approved by the local institutional research ethics committee (REC) of King Saud University, Riyadh, Saudi Arabia (approval # KSU-SE-18-40). Animals were obtained from the animal care center at college of Pharmacy, King Saud University, Riyadh, Saudi Arabia and housed in a controlled condition (23 °C and 12 h. light/dark cycle) with free access to standard chow diet and water.

2.2. Experimental design and drug treatment

Male Wistar albino rats (weighing 180–200 g) were used in our study and were randomly divided into 4 groups (10 rats per group). Control group received i.p. injection of normal saline for 28 consecutive days. Rats in LIRA group received i.p. injection of LIRA (Novo Nordisk, Denmark) dissolved in normal saline at a dose of 200 μg/kg once daily for 28 days (Mells et al. 2012; Noyan-Ashraf et al. 2009; Yang et al. 2018). GEF group, however, treated with normal saline for 7 days then with 30 mg/kg GEF (Ark Pharm, USA) by oral gavage for 21 days (Korashy et al. 2016; Rockville 2005). In LIRA + GEF group, rats were pretreated with 200 μg/kg of LIRA (i.p.) once daily for 7 days and then were co-treated with 30 mg/kg GEF orally and LIRA at dose of 200 μg/kg (once daily, (i.p.) for 21 days. Body weight was measured daily throughout the study. The dose of GEF was selected based on previous published article (Korashy et al., 2016).

On day 29, rats were anesthetized by intraperitoneal injection of ketamine/xylazine mixture then the blood was collected immediately from the heart and the serum was separated for measuring cardiac enzymes. Consequently, heart tissues were excised and washed twice with ice-cold phosphate buffer saline (PBS) and weighed. After that, heart tissues were fixed in formaldehyde solution (4%) for histopathology studies, while other tissues (n = 5) were homogenized for gene and protein expression studies and biochemical studies. Ratio of heart weight to body weight (HW/BW) was used as an indicator of myocardial mass as described previously (Katare et al., 2017; Tracy and Sander, 2011).

2.3. Heart histopathology

Heart tissues from all groups were collected at the time of euthanasia and were fixed immediately in 4% formaldehyde solution. The fixed tissues were then embedded in paraffin and thin sections of 3 μm were prepared using a microtome. Then, paraffin-embedded heart sections were deparaffinized and stained with hematoxylin and eosin (H&E). The severity of cardiac damage was evaluated blindly under an optical microscope by comparing the morphology of the cardiac cells and the nucleus of myocardial fiber cells (Ouyang et al., 2009) (Olympus BX microscope and DP72 camera).

2.4. Measurement of serum enzymes

Serum was separated from the whole blood by centrifugation of the coagulated blood at 2000*g* for 10 min at 4 °C. To measure the serum levels of different enzymes, Enzyme-Linked Immunosorbent Assay (ELISA) was used, where kits for Creatine Kinase MB Isoenzyme (CK-MB), cardiac troponin I (cTnI) and N-Terminal Pro-Brain Natriuretic Peptide (NT-proBNP) were used. Kits were purchased from G-Bioscience (MO, USA) and procedures were conducted according to the manufacturer's protocol.

2.5. Real-time quantitative polymerase chain reaction (RT-qPCR) analysis

Total cellular RNA was isolated from the heart tissues using RNeasy mini kit (Qiagen, USA) as per manufacturer's protocol. The quality and quantity of the isolated RNA were assessed using NanoDrop™ 8000 Spectrophotometer (ThermoFisher Scientific, USA). Then, the isolated RNA was reverse transcribed to cDNA

using TaqMan™ Reverse Transcription kit (ThermoFisher Scientific, USA). Changes in the expression of different genes were quantified by QuantStudio 6 Flex rea-time PCR System (ThermoFisher Scientific, USA) using SYBR green master mix (Bimake, USA) and data was normalized to β-actin, which is used as an internal control. The final concentration of the forward and reverse primers that used was 1 μM. The data acquisition was made during the extension step. Sequences of primers used in this study are listed in Table 1. All primers were purchased from Integrated DNA Technologies (IDT, Belgium). The relative levels of mRNA expression were calculated using ΔΔCt method.

2.6. Western blot analysis

Proteins were extracted from the heart tissues through homogenization in ice-cold RIPA lysis buffer (ThermoFisher Scientific, USA) that supplemented with cocktail protease inhibitor (ThermoFisher Scientific, USA). Then, the protein lysates were denatured in sample buffer (2x Laemmli buffer, Bio-Rad, USA) and heated at 95 °C for 5 min and the protein concentrations were determined by bicinchoninic acid assay (BCA) method using commercially available kit (Boster Biological Technology, USA). After that, equal amount of proteins (20–50 μg) were resolved in 10% SDS-PAGE gel, then transferred to PVDF membrane (Bio-Rad, USA) and blocked with 5% non-fat dry milk in 0.1% TBST buffer for 2 h. After blocking, membranes were incubated with rabbit anti-nuclear factor kappa B (NF-κB) polyclonal antibody, rabbit anti-superoxide dismutase (SOD) polyclonal antibody (ABclonal Technology, USA), rabbit anti-phospho-ERK1/2 monoclonal antibodies, rabbit anti-phospho-P38 monoclonal antibody, rabbit anti-phospho-SAPK/JNK monoclonal antibody, rabbit anti-phospho-Akt monoclonal antibody, rabbit anti-ERK1/2 monoclonal antibodies, rabbit anti-P38 monoclonal antibody, rabbit anti-SAPK/JNK antibody, rabbit anti-Akt monoclonal antibody and rabbit anti-cleaved poly ADP ribose polymerase (PARP) monoclonal antibody (cell signaling technology, USA) overnight at 4 °C. Then, blots were incubated with the appropriate HRP conjugated secondary antibody (ABclonal Technology, USA) for 1 h. Thereafter, membranes were visualized using chemiluminescence reagent (Merck Millipore, USA) and imaged using a Bio-Rad gel-imaging system (Bio-Rad, USA). Glyceraldehyde 3-phosphate dehydrogenase (GAPDH) monoclonal antibody (ABclonal Technology, USA) was used as a housekeeping protein. All the primary antibodies were used in dilution of 1:1000.

2.7. Measurement of superoxide dismutase (SOD) enzyme activity

Frozen heart tissues were homogenized in ice-cold lysis buffer (0.1 mM EDTA, 0.5% Triton X-100 and 50 mM potassium phosphate) and centrifuged at 12,000*g* for 5 min at 4 °C. Then, SOD enzyme activity was measured using EnzyChrom™ Superoxide Dismutase Assay Kit (BioAssay Systems, USA) as per the manufacturer's protocol.

2.8. Measurement of catalase enzyme activity

Frozen heart samples were homogenized in ice-cold PBS and centrifuged at 20,000*g* for 10 min at 4 °C. After that, catalase enzyme activity was measured using EnzyChrom™ Catalase Assay Kit (BioAssay Systems, USA) as per the manufacturer's protocol.

2.9. Measurement of cell proliferation

Viability of the human A549 lung cancer cells (ATCC, USA) was monitored for 48 h using xCELLigence real-time cell analyzer dual plate (RTCA DP, ACEA Biosciences, USA). In brief, A549 cells were seeded in 100 μL of Dulbecco's modified Eagle's medium (DMEM) in E-16 plate (ACEA Biosciences, USA) at a density of 2×10^5/well. 12 h later (when cells entered the exponential phase), GEF and GEF plus LIRA were added in the final concentration range of 1–30 μM for GEF and 5 μM & 10 μM for LIRA (Li et al., 2018; Ono et al., 2004; Zhao et al., 2018). Then, cell viability was measured after 12, 24 and 48 h and calculated using RTCA software v. 2.0.

2.10. Statistical analysis

All data are presented as mean ± SD. Statistical analyses were performed on computer using GraphPad Prism software v. 6.01 (CA, USA). Differences between multiple groups were analyzed by one-way analysis of variance (ANOVA) or two-way ANOVA, where required, followed by Tukey's *post hoc* analysis with values of $P < 0.05$ were considered significant.

3. Results

3.1. Histopathological examination

Hematoxylin and eosin (H&E) stained heart sections from the control and LIRA groups showed normal size and shape of the myocardial fibres nuclei and normal thickness of the ventricular myocardium (Fig. 1A & 1B). Conversely, stained heart sections from the GEF group revealed the presence of mild atypia and hyperchromasia in the myocardial fibres nuclei. Furthermore, heart sections from GEF group exhibited an increase in the thickness of the myocardium, which is most likely due to ventricular hypertrophy (Fig. 1C). Interestingly, heart sections from LIRA + GEF group showed normal myocardial fibres striations and nuclei similar to the sections from control and LIRA groups (Fig. 1D). To further investigate the effect of GEF treatment on the cardiac muscle, we measured the body weight (BW), heart weight (HW) and heart weight/body weight ratio (HW/BW), which we used as an indicator of cardiac hypertrophy. As shown in Table 2, we observed a considerable change in the BW in LIRA group compared to the control group. In regard to HW, a significant increase in the HW was observed in GEF treated group compared to other groups (Table 2). Furthermore, a dramatic increase in the ratio of HW/BW was noticed in the GEF-treated group compared to other groups

Table 1
List of primer sequences used in this study.

Gene	Accession umber	Primer sequences (5′→ 3′)	Product length (bp)	Reference
SOD	NM_017050.1	Forward: TTCGTTTCCTGCGGCGGCTT Reverse: TTCAGCACGCACACGGCCTT	112	Designed for this study
NF-κB	NM_199267.2	Forward: CATGCGTTTCCGTTACAAGTGCGA Reverse: TGGGTGCGTCTTAGTGGTATCTGT	85	Designed for this study
β -Actin	NM_031144.3	Forward: CCAGATCATGTTTGAGACCTTCAA Reverse: GTGGTACGACCAGAGGCATACA	87	Designed for this study

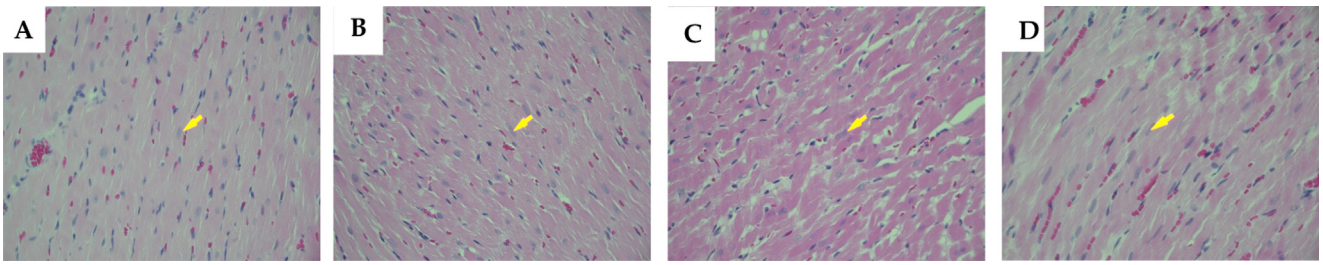

Fig. 1. Light micrographs of cardiac tissues using H&E stain. (A) Represents the normal thickness of the ventricular myocardium observed in control group. (B) Cardiac section obtained from LIRA group that shows the presence of normal myocardial fibers (arrow). (C) Represents the increase in the thickness of the myocardium and the presence of mild atypia and hyperchromasia in the myocardial fibers nuclei in GEF-treated rats. These features are induced by myocardial hypertrophy (arrow). (D) Cardiac section obtained from LIRA + GEF group that shows the normal myocardial fibers striations and nuclei (arrow). Objective magnification used was 40x. LIRA, Liraglutide; GEF, Gefitinib.

Table 2
Body weight, heart weight and heart weight to body weight ratio for rats in each group.

Parameter	Control	LIRA	GEF	LIRA + GEF
Body Weight (g)	277.9 ± 12.69	260.8 ± 7.35 *	267.9 ± 14.79	257.0 ± 7.09 $^{\$\$}$
Heart Weight (mg)	921 ± 51.16	854 ± 41.07 $^{¥}$	1079 ± 75.95 $^{\#}$	914 ± 66.52 $^{\Psi}$
Heart Weight/Body weight ratio	3.42 ± 0.10	3.50 ± 0.13 $^{¥}$	4.48 ± 0.43 $^{\#}$	3.89 ± 0.20 $^{\Psi}$

Data are presented as mean ± SD (n = 10). * Represents comparison between control and LIRA groups; where $^{*}p < 0.05$. Comparisons between GEF and control are represented by $^{\#}$; where $^{\#}p < 0.05$. Comparisons between GEF and LIRA + GEF are represented by $^{\Psi}$; where $^{\Psi}p < 0.05$. $^{\$}$ Represents the comparison between control and LIRA + GEF, where $^{\$}$ $^{\$}p < 0.01$. Comparsions between LIRA and GEF are represented by $^{¥}$, where $^{¥}p < 0.05$. LIRA, Liraglutide; GEF, Gefitinib.

(Table 2). Taken together, results suggest that LIRA treatment protect the heart against GEF-induced hypertrophy as evidenced by histopathological studies.

3.2. Effect of LIRA treatment on cardiac enzymes

To investigate whether GEF treatment is associated with cardiac damage or injury, serum levels of CK-MB, cTn-I/TNNI3 and NT-proBNP were measured in rats after 28 days of treatment. GEF treatment (30 mg/kg) resulted in a significant increase in the serum levels of cardiac enzymes compared to the control group (Fig. 2). However, the observed increase in the serum levels of CK-MB, cTn-I and NT-proBNP was diminshed in rats pretreated with 200 μg/kg LIRA (Fig. 2A, B & C, respectively). These results demonstrated that LIRA pretreatment can protect the heart from the damage induced by GEF treartment.

3.3. Antioxidant properties of LIRA

Previous studies reported that LIRA has antioxidant proterties in addition to its established antidiabetic property. Therefore, to determine whether LIRA treatment reduces the cardiac damage

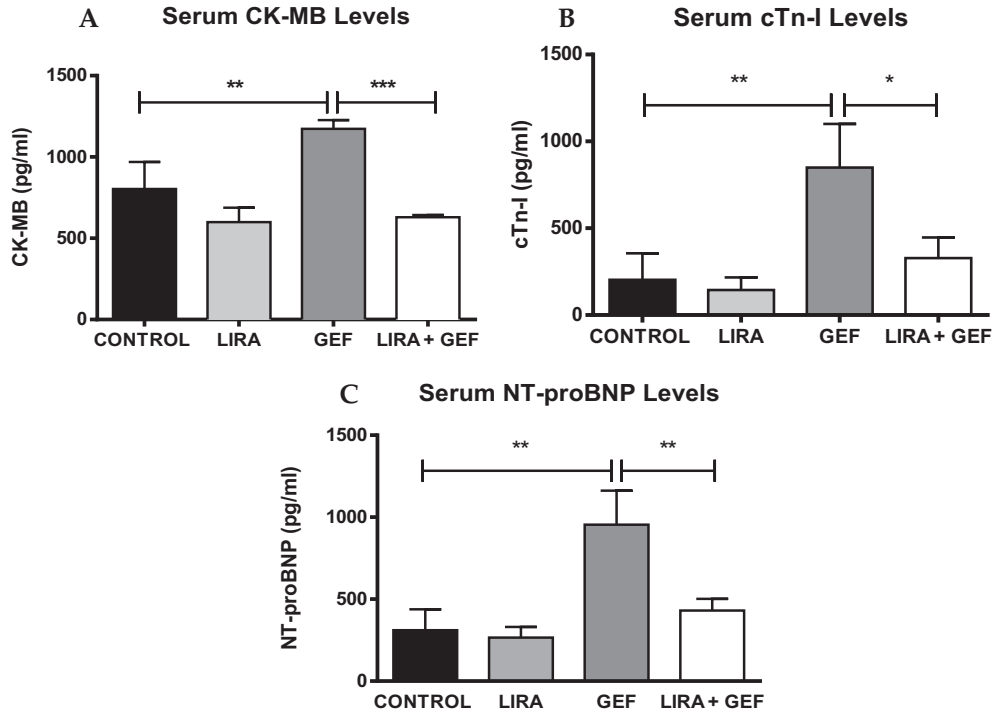

Fig. 2. Serum levels of cardiac enzymes. Serum from different groups were analyzed to measure CK-MB, cTnI & Pro-BNP levels (A, B & C, respectively). Data are presented as mean ± SD (n = 5). Where $^{*}p < 0.05$, $^{**}p < 0.01$ & $^{***}p < 0.001$. LIRA, Liraglutide; GEF, Gefitinib; CK-MB, Creatine kinase-MB; cTn-I/Tnnl3, Troponin I cardiac muscle; NT-proBNP, N-terminal pro-Brain natriuretic peptide.

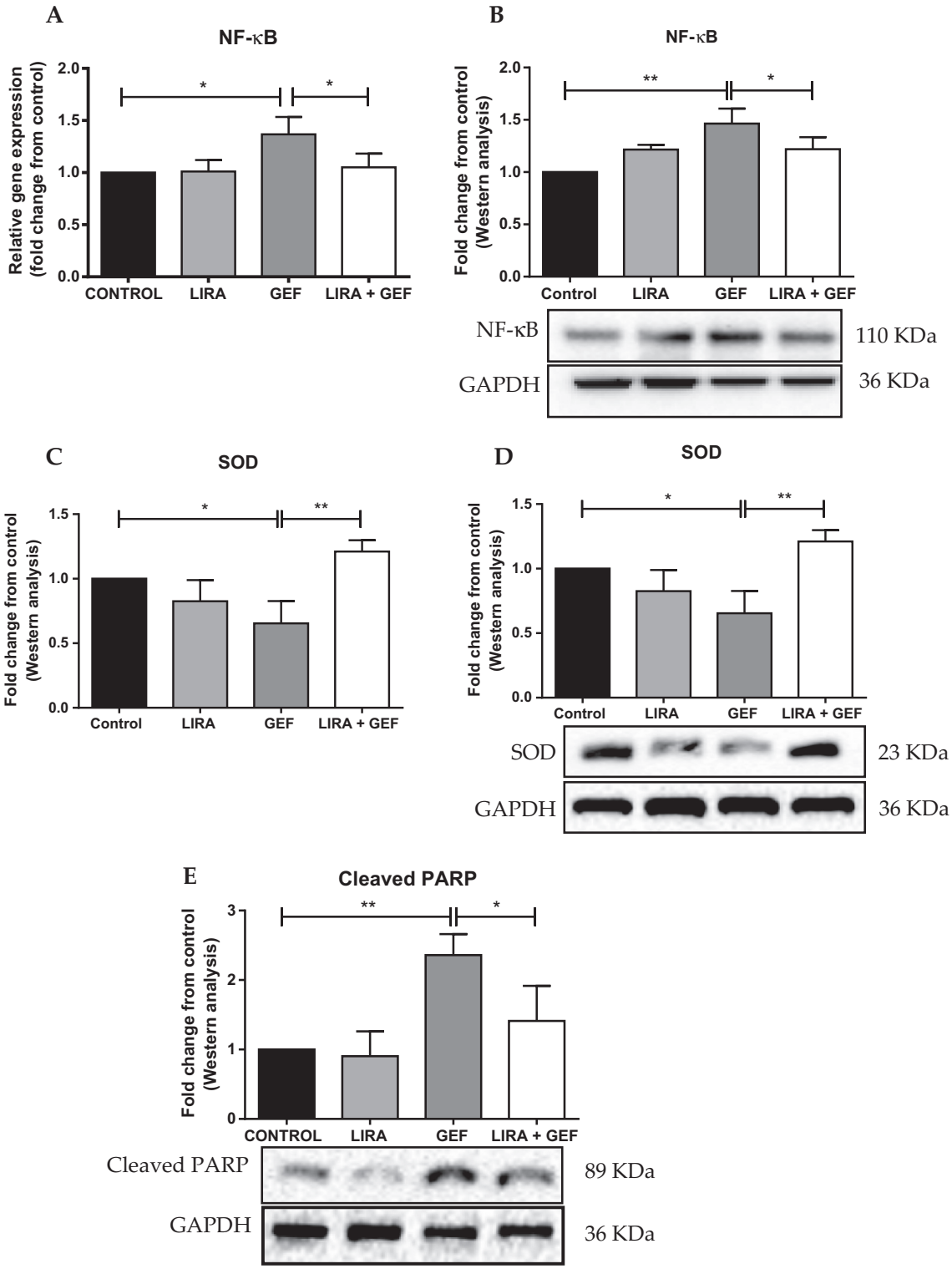

Fig. 3. Liraglutide reduces oxidative stress and induces antioxidant genes and proteins. (A) mRNA levels of NF-κB were measured by RT-PCR. (B) Representative western blot analysis of NF-κB protein levels. (C) Densitometric analysis of mRNA expression of SOD. (D) Representative immunoblot analysis of SOD protein levels. (E) Representative blot of cleaved PARP protein levels. Data are presented as mean ± SD (n = 5). Where $^{*}p < 0.05$ & $^{**}p < 0.01$. LIRA, Liraglutide; GEF, Gefitinib; NF-κB, Nuclear Factor Kappa-B; SOD, Superoxide dismutase; PARP, Poly (ADP-ribose) polymerase; GAPDH, Glyceraldehyde 3-phosphate dehydrogenase.

induced by GEF, we measured the levels of different pro-oxidant and antioxidant genes, such as NF-κB, PARP and SOD. We found that GEF treatment led to a remarkable rise in the gene and protein expressions of NF-κB compared to the control group (Fig. 3A & B). Furthermore, a notable decline in the mRNA and protein expressions of the antioxidant gene SOD was observed in the GEF treated rats (Fig. 3C & D). Strikingly, LIRA pretreatment abolished the increase in the gene and protein expressions of NF-κB that noticed in GEF-treated group (Fig. 3A & B). Moreover, when combined with GEF, LIRA markedly upregulated the gene and protein expression

levels of SOD as shown in Fig. 3C & D. Furthermore, we measured the protein levels of cleaved PARP, because it was shown that changes in the expression of PARP were associated with oxidative stress and the development of cardiotoxicity. We found that LIRA pretreament significantly mitigated the increase in cleaved PARP levels that induced by GEF (Fig. 3E).

3.4. LIRA activates prosurvival kinases in the heart

Western blot analysis revealed that GEF treatment resulted in a sharp increase in the protein levels of p-JNK and p-P38 compared to the control group (Fig. 4A & B). Additionally, the protein levels of p-ERK1/2 and p-Akt were significantly lower in the GEF treated group (Fig. 4C & D). Nonetheless, rats treated with LIRA significantly attenuated GEF-induced increase in the phosphorylation of JNK and P38 proteins (Fig. 4A & B). Furthermore, LIRA pretreatment significantly induced the protein levels of the phosphorylated form of ERK1/2 and Akt (Fig. 4C & D).

3.5. LIRA enhances the activity of antioxidant enzymes

As shown in Fig. 5A, the activity of SOD enzyme was markedly reduced in GEF-treated rats as expected. However, LIRA pretreatment restored the enzyme activity to the normal levels (Fig. 5A). On the other hand, no significant changes between groups were observed in the activity of catalase enzymes (Fig. 5B).

3.6. Effect of LIRA treatment on cell proliferation

As shown in Fig. 6, LIRA treatment did not modulate the anti-cancer activity of GEF when combined together. On the contrary, we observed more reduction in the proliferation of A549 cells treated with 5 μM of LIRA plus GEF than in cells treated with GEF alone (Fig. 6B). However, that reduction was not significant, which means that the cardioprotective effect of LIRA did not attenuate the anti-cancer activity of GEF when combined together.

4. Discussion

Our findings in the current study revealed that treatment with GEF for 28 days resulted in cardiac hypertrophy as evidenced by histopathological studies. Furthermore, we observed that GEF treated rats developed cardiac damage, that led to a significant induction of different cardiac enzymes (CK-MB, NT-proBNP and cTnI). At the cellular level, GEF treatment provoked cardiotoxicity through the increase in oxidative stress gene (NF-κB), activation of the stress-activated kinases (p-JNK and p-P38), reduction of antioxidant protein (SOD) and reduction in the prosurvival kinases (p-ERK1/2 and p-Akt). LIRA pretreatment, however, diminished these effects and led to cardioprotection through the activation of the prosurvival kinases and the induction of the antioxidant enzymes.

Tyrosine kinases (TKs) family is a group of proteins which upon stimulation leads to phosphorylation of tyrosine residue in other

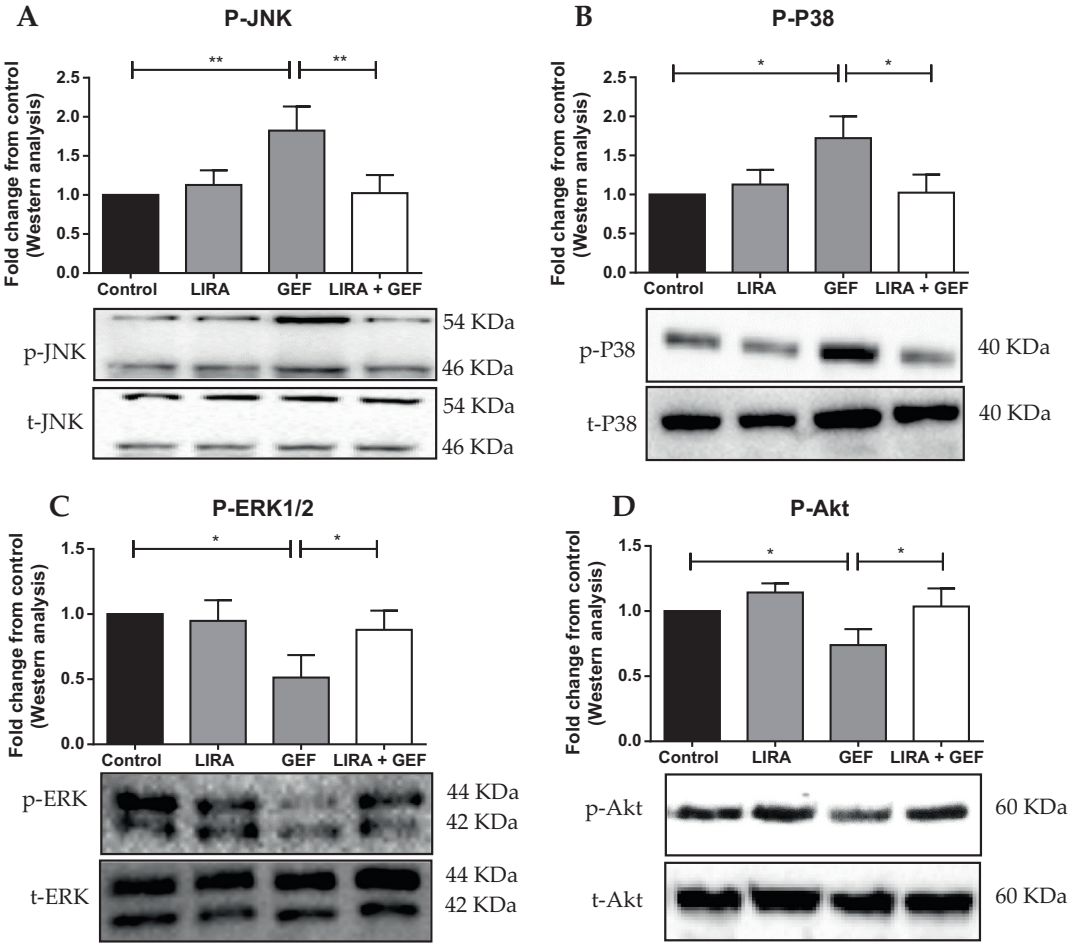

Fig. 4. Liraglutide activates protective signaling pathways in the heart. Representative western blots and relative densitometric analysis of (A) p-JNK, (B) p-P38, (C) p-ERK and (D) p-Akt protein levels. Data are presented as mean ± SD (n = 5). Where $^{*}p < 0.05$ & $^{**}p < 0.01$. LIRA, Liraglutide; GEF, Gefitinib; GAPDH, Glyceraldehyde 3-phosphate dehydrogenase.

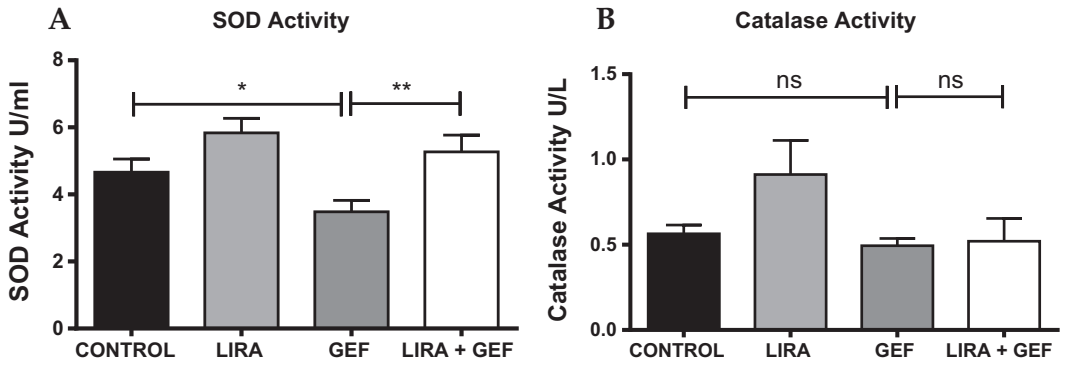

Fig. 5. Liraglutide enhances the activity of antioxidant enzymes. Biochemical analysis to measure the activity of the antioxidants SOD (A) and Catalase (B). Data are presented as mean ± SD (n = 5). Where * $p < 0.05$ & ** $p < 0.01$, while ns means no significant changes were observed ($p > 0.05$). LIRA, Liraglutide; GEF, Gefitinib; SOD, Superoxide dismutase.

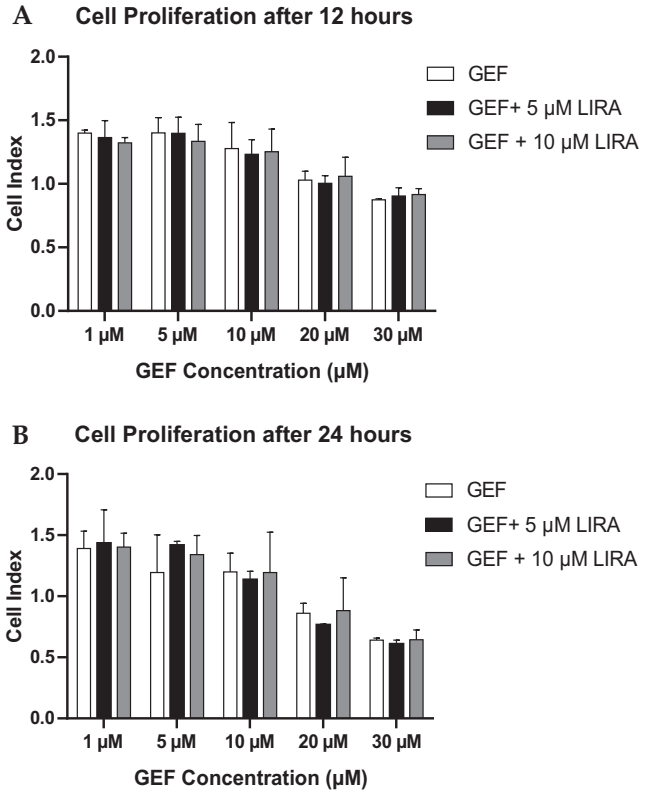

Fig. 6. Measurement of cell proliferation. A549 cells were treated with different concentrations of GEF (1 μM – 30 μM) either alone or with 5 μM and 10 μM LIRA, then the cell proliferation of A549 cells were assessed using RTCA. (A) Densitometric analysis of the average values of cell proliferation after 12 h of treatment. (B) Graphical representation of cell proliferation after 24 h of treatment. Data are presented as mean ± SD (n = 3). LIRA, Liraglutide; GEF, Gefitinib; μM, Micro Molar.

proteins within the cell. In general, TKs can be divided into RTKs and non-receptor tyrosine kinases (NRTKs) (Hervent and De Keulenaer, 2012; Orphanos et al., 2009). GEF is a competitive inhibitor of RTKs activation, especially EGFR activation. It has an extreme affinity to adenosine triphosphate (ATP) binding pocket of the EGFR. Therefore, it competes with ATP to the binding pocket (intracellular tyrosine kinase domain) of the EGFR, consequently inhibits the binding of ATP to the ATP binding pocket (Chen et al., 2008; Hervent and De Keulenaer, 2012; Segovia-Mendoza et al., 2015). This inhibition of the binding of ATP results in inhibition of receptor autophosphorylation, which block the downstream signal transduction resulting in inhibition of tumor growth, proliferation and differentiation and eventually induction of apoptosis in cancerous cells (Segovia-Mendoza et al., 2015).

It has been reported that GEF treatment induced cardiomyopathy in 56-year-old patient with EGFR-mutated NSCLC. Furthermore, GEF was associated with recurrent myocardial infarction in patient with metastatic carcinoid tumor (Lynch et al., 2011). Moreover, it was shown that GEF treatment resulted in cardiotoxicity both *in-vitro* and *in-vivo* (Korashy et al., 2016). In that study, researchers reported that treating rats for 21 consecutive days with 30 mg/kg GEF significantly elevated cardiac enzymes and induced the expression of oxidative stress markers, which eventually resulted in cardiac hypertrophy and induction of apoptotic markers. They have reported that the induction of apoptotic markers was associated with GEF-induced hypertrophy. Previous study defined the cardiac hypertrophy as an increase in the size of the cardiac cells that leads to enlargement of the heart (Dorn et al., 2003). Furthermore, it has been shown that serum biomarkers, such as natriuretic peptides and cardiac troponin, demonstrate an efficient and novel tool that can reliably estimate the potential and severity of cardiotoxicity induced by anticancer agents (Tian et al., 2014). Our findings in the present study were consistent with previous reports as we showed that GEF treatment resulted in cardiac hypertrophy as validated by histopathology studies. Furthermore, GEF-induced cardiac damage was confirmed by measuring the serum levels of different cardiac enzymes and the levels of pro-oxidant and antioxidant genes in rats treated with GEF for 21 days. At the cellular level, we demonstrated that GEF led to activation of the phosphorylated form of JNK and P38 proteins, which are known to be induced in response to cellular stresses. In contrast, the activation of the pro-survival kinases was attenuated in GEF-treated rats. These findings were in accordance with previous studies as it has been reported that GEF attenuated the activity of ErbB2 and ErbB3 resulting in significant inhibition of the intracellular signaling pathways, such as MAPKs (ERK1/2) and Akt (Cragg et al., 2007; Segovia-Mendoza et al., 2015; Yang et al., 2017). Although inhibition of the MAPK and Akt signaling pathways is crucial for treating cancer cells, activation of these pathways is the main mechanism that leads to drug-resistant, which can result in reduced response to the anti-cancer drug, and consequently tumor progression. Based on that, different agents that inhibit the activation of MAPK and PI3K/Akt signaling pathways are now in clinical trials (Jiao et al., 2018; Montor et al., 2018).

LIRA is glucagon-like peptide-1 (GLP-1) receptor agonist that is used to effectively to treat patients with type 2 diabetes mellitus either as monotherapy or as a combination with other antidiabetic medications. Structurally, it is highly similar (almost 97%) to

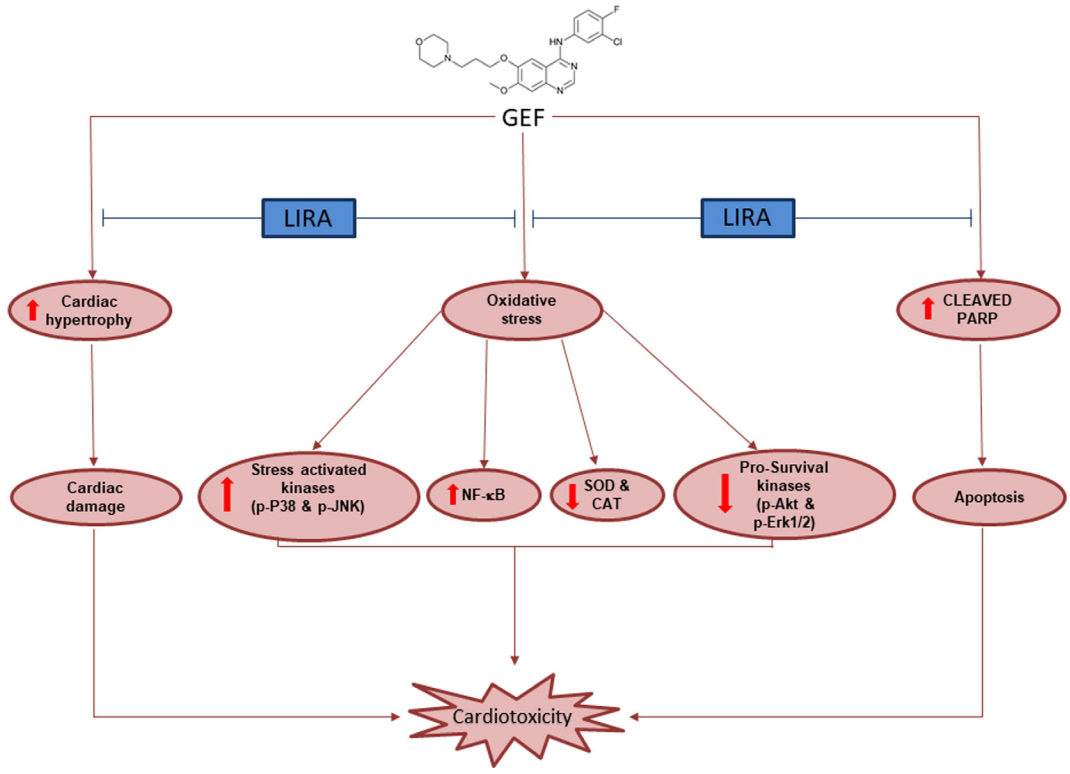

Fig. 7. Schematic diagram of the cardioprotective effect of LIRA against GEF-induced cardiotoxicity. LIRA, Liraglutide; GEF, Gefitinib; SOD, Superoxide dismutase; CAT, Catalase; NF-κB, Nuclear Factor Kappa-B.

human GLP-1 amino acid sequence (Deng et al., 2018; Garber, 2011). Myriad of studies documented the cardioprotective effect of LIRA against different insult (Dhatariya et al., 2018; Garber, 2011; Marso et al., 2016; Noyan-Ashraf et al., 2009; Verma et al., 2018; Zhang et al., 2018). Recently, it has been shown that the rates of deaths from cardiovascular diseases were remarkably lower in patient with type 2 diabetes mellitus who treated with LIRA (Marso et al., 2016). In that randomized double-blind trial (LEADER trial), LIRA treatment reduced the rates of hospitalization for heart failure, non-fatal stroke, non-fatal myocardial infarction and the death from non-cardiovascular causes in type 2 diabetic patients. The reduction in the rates of deaths from cardiovascular causes among type 2 diabetic patients was shown to be independent of reduction in hypoglycemia (Zinman et al., 2018). In animal model, Noyan-Ashraf and his colleagues reported that LIRA offered cardioprotection and improved the cardiac function in diabetic mice subjected to experimental ischemia (Noyan-Ashraf et al., 2009). In their study, they pre-treated the mice with LIRA for 7 days, then subject the mice to experimental ischemia. 28 days post MI, they found that LIRA pretreatment notably improved survival, reduced the infarct size, reduced the cardiac rupture and improved cardiac function. These beneficial effects were reported to be independent of reduction in body weight (Noyan-Ashraf et al., 2009). It has been suggested that the protective effects of LIRA is mainly due to its antioxidant property as it has been shown that LIRA treatment reduced oxidative stress and restored the antioxidant enzymes activity (Bianchi et al., 2019; Deng et al., 2018; Rizzo et al., 2015; Zhu et al., 2015). Consistent with previous studies, we reported that pretreatment with LIRA protected the heart from GEF-induced cardiac damage and apoptosis as confirmed by histopathology studies. Furthermore, LIRA maintained the serum levels of cTnI, CK-MB and NT-proBNP within normal levels, which are shown to be significantly induced in response to GEF treatment. To further investigate the antioxidant property of LIRA, we measured the expression and the activity of SOD and we demonstrated that LIRA induced SOD gene and protein expression and restored its activity. Furthermore, the induction of pro-oxidant genes that observed in GEF group was mitigated in LIRA pretreated group, suggesting that the protective effect of LIRA is mediated through its antioxidant property.

Many studies reported that activation of ERK1/2 and Akt can efficiently diminish oxidative stress by controlling the expression of different genes. The increase in oxidative stress, however, can in turn generate more reactive oxygen species (ROS), which inhibit the phosphorylation of ERK1/2 and Akt (Wiciński et al., 2019; Zhang et al., 2015; Zhu et al., 2016). In cardiac myocytes, activation of ERK1/2 and Akt and inhibition of the phosphorylation of P38 and JNK were shown to induce protection against myocardial ischemia–reperfusion (IR) injury (Vassalli et al., 2012). In one study, activation of P38 was shown to alleviate the protective effect induced by insulin against IR injury. Furthermore, it was reported that activation of p-JNK resulted in mitochondrial damage and apoptosis and adult rat cardiomyocytes in response to oxidative stress (Vassalli et al., 2012). Activation of Akt signaling pathway is fundamental for the protective effect of LIRA (Zhu et al., 2016). It has been reported that activation of Akt and ERK signaling pathways reduced apoptosis and oxidative damage through the inhibition of NF-KB (Wiciński et al., 2019). Furthermore, it has been shown that the protective effect of LIRA in diabetic mice subjected to myocardial IR injury was chiefly mediated through the activation of Akt (Noyan-Ashraf et al., 2009). In accordance with previous studies, our results showed that LIRA pretreatment stimulated the phosphorylation of Akt and ERK1/2 proteins and inhibited the activation of stress-activated kinases, P-JNK and p-P38, which in turn protected the heart against the damage induced by GEF.

Although LIRA has been reported to inhibit proliferation and induce apoptosis in MCF-7 and HepG2 cells, little is known regarding the effect of LIRA in A549 cells. In order to investigate

whether the use of LIRA in combination with GEF has any effects on the anti-cancer activity of GEF, we measured the proliferation of A549 cells for 48 h. We found that LIRA did not attenuate the anti-cancer activity of GEF when combined together, which indicates the need for further studies to assess the efficacy and safety of such combination.

5. Conclusion

In the present study, we demonstrated that treatment with GEF resulted in cardiac hypertrophy and induction of cardiac enzymes (CK-MB and cTnI). Furthermore, GEF treatment led to increase in oxidative stress genes, reduction of antioxidant proteins and reduction in the prosurvival kinases. LIRA pretreatment, however, diminished these effects and led to cardioprotection through the activation of the prosurvival kinases (Fig. 7). These findings expand our knowledge about the cardioprotective effect of LIRA, which can help to further investigate the mechanism of protection induced by GLP-1 agonists.

Declaration of Competing Interest

The authors declare that they have no known competing financial interests or personal relationships that could have appeared to influence the work reported in this paper.

Acknowledgments

The authors extend their appreciation to the Deanship of Scientific Research at King Saud University for funding this work through the Research Project No. NFG-7-18-02-29.

References

Bianchi, M., D'Oria, V., Braghini, M.R., Petrini, S., Manco, M., 2019. Liraglutide treatment ameliorates neurotoxicity induced by stable silencing of Pin1. Int. J. Mol. Sci. 20.

Briyal, S., Shah, S., Gulati, A., 2014. Neuroprotective and anti-apoptotic effects of liraglutide in the rat brain following focal cerebral ischemia. Neuroscience 281, 269–281.

Chen, M.H., Kerkela, R., Force, T., 2008. Mechanisms of cardiac dysfunction associated with tyrosine kinase inhibitor cancer therapeutics. Circulation 118, 84–95.

Chen, Z., Gibson, T.B., Robinson, F., Silvestro, L., Pearson, G., Xu, B., Wright, A., Vanderbilt, C., Cobb, M.H., 2001. MAP kinases. Chem. Rev. 101, 2449–2476.

Cragg, M.S., Kuroda, J., Puthalakath, H., Huang, D.C., Strasser, A., 2007. Gefitinib-induced killing of NSCLC cell lines expressing mutant EGFR requires BIM and can be enhanced by BH3 mimetics. PLoS Med. 4, 1681–1689. discussion 1690.

Deng, C., Cao, J., Han, J., Li, J., Li, Z., Shi, N., He, J., 2018. Liraglutide activates the Nrf2/HO-1 antioxidant pathway and protects brain nerve cells against cerebral ischemia in diabetic rats. Comput. Intell. Neurosci. 2018, 3094504.

Dhatariya, K., Bain, S.C., Buse, J.B., Simpson, R., Tarnow, L., Kaltoft, M.S., Stellfeld, M., Tornoe, K., Pratley, R.E. and Investigators, L.P.C.O.B.O.T.L.T., 2018. The impact of liraglutide on diabetes-related foot ulceration and associated complications in patients with type 2 diabetes at high risk for cardiovascular events: results from the LEADER Trial. Diabetes Care 41, 2229–2235.

Dorn 2nd, G.W., Robbins, J., Sugden, P.H., 2003. Phenotyping hypertrophy: eschew obfuscation. Circ. Res. 92, 1171–1175.

Garber, A.J., 2011. Long-acting glucagon-like peptide 1 receptor agonists: a review of their efficacy and tolerability. Diabetes Care 34 (Suppl 2), S279–284.

Guo, J., Li, C., Yang, C., Li, B., Wei, J., Lin, Y., Ye, P., Hu, G., Li, J., 2018. Liraglutide reduces hepatic glucolipotoxicityinduced liver cell apoptosis through NRF2 signaling in Zucker diabetic fatty rats. Mol. Med. Rep. 17, 8316–8324.

Hervent, A.S., De Keulenaer, G.W., 2012. Molecular mechanisms of cardiotoxicity induced by ErbB receptor inhibitor cancer therapeutics. Int. J. Mol. Sci. 13, 12268–12286.

Jiao, Q., Bi, L., Ren, Y., Song, S., Wang, Q., Wang, Y.S., 2018. Advances in studies of tyrosine kinase inhibitors and their acquired resistance. Mol. Cancer 17, 36.

Katare, P.B., Bagul, P.K., Dinda, A.K., Banerjee, S.K., 2017. Toll-like receptor 4 inhibition improves oxidative stress and mitochondrial health in isoproterenol-induced cardiac hypertrophy in rats. Front. Immunol. 8, 719.

Kazandjian, D., Blumenthal, G.M., Yuan, W., He, K., Keegan, P., Pazdur, R., 2016. FDA approval of gefitinib for the treatment of patients with metastatic EGFR mutation-positive non-small cell lung cancer. Clin. Cancer Res. 22, 1307–1312.

Korashy, H.M., Attafi, I.M., Ansari, M.A., Assiri, M.A., Belali, O.M., Ahmad, S.F., Al-Alallah, I.A., Anazi, F.E., Alhaider, A.A., 2016. Molecular mechanisms of cardiotoxicity of gefitinib in vivo and in vitro rat cardiomyocyte: Role of apoptosis and oxidative stress. Toxicol. Lett. 252, 50–61.

Krawczyk, P., Kowalski, D.M., Ramlau, R., Kalinka-Warzocha, E., Winiarczyk, K., Stencel, K., Powrozek, T., Reszka, K., Wojas-Krawczyk, K., Bryl, M., Wojcik-Superczynska, M., Glogowski, M., Barinow-Wojewodzki, A., Milanowski, J., Krzakowski, M., 2017. Comparison of the effectiveness of erlotinib, gefitinib, and afatinib for treatment of non-small cell lung cancer in patients with common and rare EGFR gene mutations. Oncol. Lett. 13, 4433–4444.

Kyriakis, J.M., Avruch, J., 2001. Mammalian mitogen-activated protein kinase signal transduction pathways activated by stress and inflammation. Physiol. Rev. 81, 807–869.

Li, Y.L., Hu, X., Li, Q.Y., Wang, F., Zhang, B., Ding, K., Tan, B.Q., Lin, N.M., Zhang, C., 2018. Shikonin sensitizes wildtype EGFR NSCLC cells to erlotinib and gefitinib therapy. Mol. Med. Rep. 18, 3882–3890.

Lynch Jr., D.R., Kickler, T.S., Rade, J.J., 2011. Recurrent myocardial infarction associated with gefitinib therapy. J. Thromb. Thrombolysis 32, 120–124.

Marso, S.P., Daniels, G.H., Brown-Frandsen, K., Kristensen, P., Mann, J.F., Nauck, M.A., Nissen, S.E., Pocock, S., Poulter, N.R., Ravn, L.S., Steinberg, W.M., Stockner, M., Zinman, B., Bergenstal, R.M., Buse, J.B., Committee, L.S., Investigators, L.T., 2016. Liraglutide and cardiovascular outcomes in type 2 diabetes. N. Engl. J. Med. 375, 311–322.

Mells, J.E., Fu, P.P., Sharma, S., Olson, D., Cheng, L., Handy, J.A., Saxena, N.K., Sorescu, D., Anania, F.A., 2012. Glp-1 analog, liraglutide, ameliorates hepatic steatosis and cardiac hypertrophy in C57BL/6J mice fed a Western diet. Am. J. Physiol. Gastrointest. Liver Physiol. 302, G225–235.

Montor, W.R., Salas, A., Melo, F.H.M., 2018. Receptor tyrosine kinases and downstream pathways as druggable targets for cancer treatment: the current arsenal of inhibitors. Mol. Cancer 17, 55.

Noyan-Ashraf, M.H., Momen, M.A., Ban, K., Sadi, A.M., Zhou, Y.Q., Riazi, A.M., Baggio, L.L., Henkelman, R.M., Husain, M., Drucker, D.J., 2009. GLP-1R agonist liraglutide activates cytoprotective pathways and improves outcomes after experimental myocardial infarction in mice. Diabetes 58, 975–983.

Ono, M., Hirata, A., Kometani, T., Miyagawa, M., Ueda, S., Kinoshita, H., Fujii, T., Kuwano, M., 2004. Sensitivity to gefitinib (Iressa, ZD1839) in non-small cell lung cancer cell lines correlates with dependence on the epidermal growth factor (EGF) receptor/extracellular signal-regulated kinase 1/2 and EGF receptor/Akt pathway for proliferation. Mol. Cancer Ther. 3, 465–472.

Orphanos, G.S., Ioannidis, G.N., Ardavanis, A.G., 2009. Cardiotoxicity induced by tyrosine kinase inhibitors. Acta Oncol. 48, 964–970.

Ouyang, J., Guzman, M., Desoto-Lapaix, F., Pincus, M.R., Wieczorek, R., 2009. Utility of desmin and a Masson's trichrome method to detect early acute myocardial infarction in autopsy tissues. Int. J. Clin. Exp. Pathol. 3, 98–105.

Rizzo, M., Abate, N., Chandalia, M., Rizvi, A.A., Giglio, R.V., Nikolic, D., Marino Gammazza, A., Barbagallo, I., Isenovic, E.R., Banach, M., Montalto, G., Li Volti, G., 2015. Liraglutide reduces oxidative stress and restores heme oxygenase-1 and ghrelin levels in patients with type 2 diabetes: a prospective pilot study. J. Clin. Endocrinol. Metab. 100, 603–606.

Rockville, M., 2005. US Food and Drug Administration; 2005. USFDA. Guidance for Industry: Estimating the Maximum Safe Starting Dose in Adult Healthy Volunteer.

Roux, P.P., Blenis, J., 2004. ERK and p38 MAPK-activated protein kinases: a family of protein kinases with diverse biological functions. Microbiol. Mol. Biol. Rev. 68, 320–344.

Schlessinger, J., 2000. Cell signaling by receptor tyrosine kinases. Cell 103, 211–225.

Schlessinger, J., 2014. Receptor tyrosine kinases: legacy of the first two decades. Cold Spring Harb. Perspect. Biol. 6.

Segovia-Mendoza, M., Gonzalez-Gonzalez, M.E., Barrera, D., Diaz, L., Garcia-Becerra, R., 2015. Efficacy and mechanism of action of the tyrosine kinase inhibitors gefitinib, lapatinib and neratinib in the treatment of HER2-positive breast cancer: preclinical and clinical evidence. Am. J. Cancer Res. 5, 2531–2561.

Tian, S., Hirshfield, K.M., Jabbour, S.K., Toppmeyer, D., Haffty, B.G., Khan, A.J., Goyal, S., 2014. Serum biomarkers for the detection of cardiac toxicity after chemotherapy and radiation therapy in breast cancer patients. Front. Oncol. 4, 277.

Tracy, R.E., Sander, G.E., 2011. Histologically measured cardiomyocyte hypertrophy correlates with body height as strongly as with body mass index. Cardiol. Res. Pract. 2011, 658958.

Vassalli, G., Milano, G., Moccetti, T., 2012. Role of mitogen-activated protein kinases in myocardial ischemia-reperfusion injury during heart transplantation. J. Transplant 2012, 928954.

Verma, S., Bhatt, D.L., Bain, S.C., Buse, J.B., Mann, J.F.E., Marso, S.P., Nauck, M.A., Poulter, N.R., Pratley, R.E., Zinman, B., Michelsen, M.M., Monk Fries, T., Rasmussen, S., Leiter, L.A. and Investigators, L.P.C.O.B.O.T.L.T., 2018. Effect of liraglutide on cardiovascular events in patients with type 2 diabetes mellitus and polyvascular disease: results of the LEADER trial. Circulation 137, 2179–2183.

Wicinski, M., Socha, M., Malinowski, B., Wodkiewicz, E., Walczak, M., Gorski, K., Slupski, M., Pawlak-Osinska, K., 2019. Liraglutide and its neuroprotective properties-focus on possible biochemical mechanisms in Alzheimer's disease and cerebral ischemic events. Int. J. Mol. Sci. 20.

Yang, Y., Fang, H., Xu, G., Zhen, Y., Zhang, Y., Tian, J., Zhang, D., Zhang, G., Xu, J., 2018. Liraglutide improves cognitive impairment via the AMPK and PI3K/Akt signaling pathways in type 2 diabetic rats. Mol. Med. Rep. 18, 2449–2457.

Yang, Z., Hackshaw, A., Feng, Q., Fu, X., Zhang, Y., Mao, C., Tang, J., 2017. Comparison of gefitinib, erlotinib and afatinib in non-small cell lung cancer: A meta-analysis. Int. J. Cancer 140, 2805–2819.

Zhang, Q., Xiao, X., Zheng, J., Li, M., Yu, M., Ping, F., Wang, T., Wang, X., 2018. Liraglutide protects cardiac function in diabetic rats through the PPARalpha pathway. Biosci. Rep.

Zhang, Y., Hu, S.Y., Yin, T., Tian, F., Wang, S., Zhang, Y., Chen, Y., 2015. Liraglutide promotes proliferation and migration of cardiac microvascular endothelial cells through PI3K/Akt and MAPK/ERK signaling pathways. Nan Fang Yi Ke Da Xue Xue Bao 35, 1221–1226.

Zhao, W., Zhang, X., Zhou, Z., Sun, B., Gu, W., Liu, J., Zhang, H., 2018. Liraglutide inhibits the proliferation and promotes the apoptosis of MCF-7 human breast cancer cells through downregulation of microRNA-27a expression. Mol. Med. Rep. 17, 5202–5212.

Zhu, H., Zhang, Y., Shi, Z., Lu, D., Li, T., Ding, Y., Ruan, Y., Xu, A., 2016. The neuroprotection of liraglutide against ischaemia-induced apoptosis through the activation of the PI3K/AKT and MAPK pathways. Sci. Rep. 6, 26859.

Zhu, T., Wu, X.L., Zhang, W., Xiao, M., 2015. Glucagon like peptide-1 (GLP-1) modulates OVA-induced airway inflammation and mucus secretion involving a Protein Kinase A (PKA)-dependent nuclear factor-kappaB (NF-kappaB) signaling pathway in mice. Int. J. Mol. Sci. 16, 20195–20211.

Zinman, B., Marso, S.P., Christiansen, E., Calanna, S., Rasmussen, S., Buse, J.B. and Investigators, L.P.C.O.B.O.T.L.T., 2018. Hypoglycemia, Cardiovascular Outcomes, and Death: The LEADER Experience. Diabetes Care 41, 1783–1791.